Journal of Materials Chemistry

Cite this: J. Mater. Chem., 2012, 22, 15530

www.rsc.org/materials

COMMUNICATION

Mussel foot protein-1 (mcfp-1) interaction with titania surfaces†

Dong Soo Hwang,‡*[a] Matthew J. Harrington,‡[b] Qingye Lu,[c] Admir Masic,[b] Hongbo Zeng*[c] and J. Herbert Waite*[d]

Received 19th April 2012, Accepted 25th June 2012
DOI: 10.1039/c2jm32439c

Marine mussels utilize a variety of DOPA-rich proteins for purposes of underwater adhesion, as well as for creating hard and flexible surface coatings for their tough and stretchy byssal fibers. In the present study, moderately strong, yet reversible wet adhesion between the protective mussel coating protein, mcfp-1, and amorphous titania was measured with a surface force apparatus (SFA). In parallel, resonance Raman spectroscopy was employed to identify the presence of bidentate DOPA–Ti coordination bonds at the TiO_2–protein interface, suggesting that catechol–TiO_2 complexation contributes to the observed reversible wet adhesion. These results have important implications for the design of protective coatings on TiO_2.

Titanium based materials are much in favor for dental and orthopedic implants.[1,2] They are lightweight with excellent mechanical properties and demonstrate corrosion resistance in a wide range of physiological fluids. Given the additional potential for applications beyond hard tissue implants, considerable research is being directed to customize coatings for titania surfaces that are anti-fouling, non-inflammatory, and capable of inducing specific cell growth. Bioactive coatings engineered for titania to date, however, have met with limited success due largely to deterioration by endogenous enzymes, protein fouling, inflammation *via* the innate immune system, or mechanical wear due to friction and erosion.[2,3]

Recently, a naturally occurring high performance coating has been identified in the byssal threads of marine mussels (*Mytilus* species) where it provides a thin protective cuticle over the collagenous matrix of each byssal thread.[4,5] Mechanical analysis of the byssal cuticle found it combined two critical properties that rarely coexist in the same material: high hardness (as well as stiffness) and high extensibility. Cuticle hardness is comparable to the hardness of epoxies, which are widely used as industrial coatings. However, in contrast to epoxy extensibilities of <5%, cuticle extensibility exceeds 70% and is reversible.[4,5] Additionally, the byssus cuticle apparently resists degradation by marine microbes and shows greatly reduced immunogenicity upon cross-linking.[6,7]

The byssal cuticle composition appears simple – a single protein – mussel foot protein-1 (mfp-1) – and micro-molar concentrations of metal ions, notably Fe^{3+} and Ca^{2+}.[5] Mcfp-1 from *M. californianus* has a mass of about 88 kDa and consists largely of tandem repeats of a decapeptide [PKISYO*OTY*K], in which O, O*, and Y* denote *trans*-4-hydroxyproline, *trans*-2,3, *cis*-3,4-dihydroxyproline, and 3,4-dihydroxyphenylalanine (DOPA), respectively.[5] In solution at pH 7.5, purified mcfp-1 forms stable tris- and bis-catecholate complexes with Fe^{3+} ($\log K_s \sim 43$) by means of its DOPA side chains.[8,9] Recent analyses by resonance Raman microscopy have directly confirmed the presence of catecholato–Fe^{3+} complexes in the cuticle, and studies employing the surface forces apparatus (SFA) have revealed robust and reversible bridging between monomolecular mefp-1 (from *M. edulis*) films in aqueous buffer mediated by catecholato–Fe^{3+} complexes.[10,11] At an adhesion energy, $E_{ad} \approx -4.3$ mJ m^{-2}, this bridging approaches the strongest known noncovalent protein–ligand interaction, *i.e.* avidin–biotin ($E_{ad} \approx -10$ mJ m^{-2}).[11]

The catechol moiety of DOPA is known to form strong, reversible interactions with Fe^{3+} ions, but also binds iron and titanium hydroxides on hydrated solid steel and titania surfaces, respectively.[10–13] However, the strength of the DOPA–TiO_2 interaction has been thrown into question by conflicting AFM-based measurements ranging from 800 pN to 67 pN per bond but spectroscopic methods were used.[14,15] To better understand the TiO_2–DOPA interaction, mechanical tests should ideally be performed in parallel with a spectroscopic method that can determine the interfacial chemistry. Therefore, the adhesion between mcfp-1 and TiO_2 was investigated and compared to mcfp-1 adhesion on mica in the surface forces apparatus (SFA), and confocal resonance Raman microscopy was used to probe the interfacial chemistry.

The adhesion of mcfp-1 to bare mica differs significantly from adhesion to TiO_2 (asymmetric) (Fig. 1). The ability of mcfp-1 to adhere to mica or TiO_2 surfaces is revealed by the force–distance curves (f–d curve) and by the repulsion associated with an initial approach to the hard wall, the separation distance of the two surfaces, which does not appear to change with the increase of the normal load, followed by separation of the surfaces. Adsorption of

[a]*POSTECH Ocean Science and Technology Institute, Pohang University of Science and Technology, Pohang 790784, South Korea. E-mail: dshwang@postech.ac.kr*
[b]*Department of Biomaterials, Max Planck Institute for Colloids and Interfaces, 14424 Potsdam-Golm, Germany*
[c]*Department of Chemical Engineering, University of Alberta, Canada. E-mail: hongbo.zeng@ualberta.ca*
[d]*Materials Research Laboratory, University of California, Santa Barbara, California 93106, USA. E-mail: waite@lifesci.ucsb.edu*
† Electronic supplementary information (ESI) available. See DOI: 10.1039/c2jm32439c
‡ D.S. Hwang and Matthew J. Harrington contributed equally to this work.

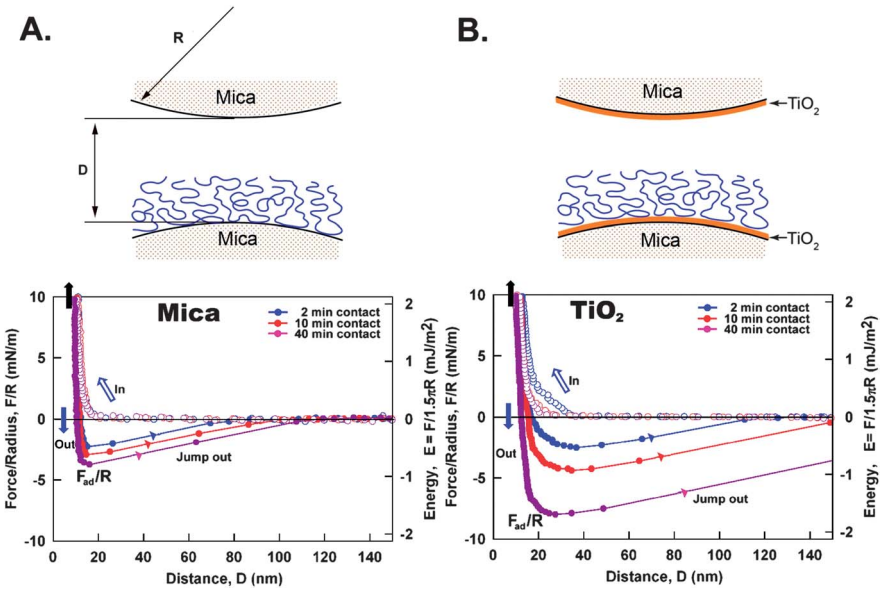

Fig. 1 Adhesion forces of mcfp-1 films on mica (A) and on TiO_2 (B) as a function of contact time at pH 5.5. *D* is the distance between two bare surfaces. Open circle – approach, closed circle – separation. The measured force, F/R (normalized by the radius of the surface, *R*), is denoted in the left ordinate, whereas the corresponding interaction energy per unit area, *E*, between two flat surfaces, defined by $E = F/1.5\pi R$, is on the right. The hard wall corresponds to the thickness of compressed protein film and is indicated by the black arrows (top left corner).

mcfp-1 to mica or TiO_2 was confirmed by the hard wall distance shift (~10 nm), corresponding to the thickness of compressed mcfp-1 film, evident from the FECO signal shift and shape changes as previously shown.[16,17] Because the hydrodynamic radius (R_H) of mcfp-1 measured by dynamic light scattering (DLS) in 0.1 M sodium acetate, pH 5.0, was ~8 nm, we deduce mcfp-1 films on mica and TiO_2 to be roughly monomolecular in thickness. Short contact times (~2 min) are sufficient to enable mcfp-1 binding to both surfaces. Adhesion to TiO_2 is roughly double that of mica and is consistent with previous SFA experiments using DOPA-containing polymers.[17] With longer contact times (~40 min), asymmetric mcfp-1 films showed higher adhesion on both mica and TiO_2 surfaces. Following several approach/separation cycles with brief contacts (~2 min each), a cycle with a 40 min contact time showed reproducible adhesion to both surfaces without significant loss in adhesion energy. In other words, mcfp-1 adhesion to mica or TiO_2 is reversible in aqueous buffer and once the mcfp-1 films have rearranged for adhesion during the contact compression.

The root mean square (rms) roughness values determined by AFM are 0.2 nm for mica and 0.8 nm for mica-supported TiO_2 (Fig. S1†). Perhaps the higher surface roughness of TiO_2 reduced the number of effective "binding sites" with the mcfp-1 film; it should be noted that as the R_H of mcfp-1 is 8 nm with a stiff repeated decapeptide unit, mcfp-1 chains are not likely to adapt well to the granular textured (rough) patterns of the opposing TiO_2 surface (Fig. S1†), leading to a reduced number of effective "bonding sites" on the TiO_2 surface than on molecularly smooth mica under the same applied pressures during force measurements. Previous studies on the roughness effects on adhesion of both soft polymer films and hard gypsum crystal surfaces showed similar results and reduced adhesion with increasing the rms surface roughness;[18–20] thus the actual adhesion energy between molecularly smooth TiO_2 and mcfp-1 is likely stronger than the SFA measurements obtained here. If TiO_2 of the same roughness (~0.2 nm) as mica was used, one would expect the mcfp-1 interaction with titania to increase and the difference between the mcfp-1–TiO_2 interaction and the mcfp-1–mica interaction to be greater.[18–20]

In previous experiments, the adhesion energy of DOPA-containing proteins to mica surfaces with added oxidants or at higher pH was significantly reduced by the oxidation of DOPA (>90%) to DOPA quinone.[21,22] Similarly, if adhesion between TiO_2 and mcfp-1 required DOPA-mediated interactions, adhesion would be diminished by treatments such as sodium periodate or increased pH that favor quinone formation. Addition of periodate eliminated the adhesion between mcfp-1 and TiO_2 after an intermediate contact time (~10 minutes) as shown in Fig. 2A. But the loss in adhesion with periodate treatment was not restored by reduction of mcfp-1 with excess anti-oxidant, such as ascorbic acid (data not shown), in contrast to the reductive rescue of adhesion of mfp-3 on mica.[21,22] Increasing the buffer pH from 5.5 to 7.5 also abolished measurable adhesion between mcfp-1 and TiO_2. The hard wall distance increased from ~10 nm to ~30 nm, suggesting mcfp-1 film expansion at higher pH. A previous observation of mfp-3 film expansion following DOPA oxidation was attributed to the tautomerization of DOPA quinone to Δ-DOPA.[21] DOPA oxidation by periodate or at higher pH also contributes to a loss in adhesion to TiO_2 by synthetic DOPA-containing polymers.[17] These data support the interpretation that adhesion between TiO_2 and mcfp-1 mainly comes from interactions between the catecholic moiety of DOPA and TiO_2.

It was previously demonstrated using vibrational spectroscopy that in acidic solutions of catechol and TiO_2 anatase nanoparticles, the dominant mode of adsorption was bidentate chelation by the fully dissociated catecholate form.[23] In order to investigate the nature of the chemical interaction between DOPA side chains of mcfp-1 and the TiO_2 surface, confocal Raman spectroscopy was employed, as described previously for mfp-1–Fe^{3+} interactions.[10,11,24] Spectra acquired from control samples of TiO_2-coated mica show a large broad band in the low energy region (200–800 cm^{-1}) indicating that the TiO_2 is primarily amorphous (Fig. 3A, black line).[25] In contrast,

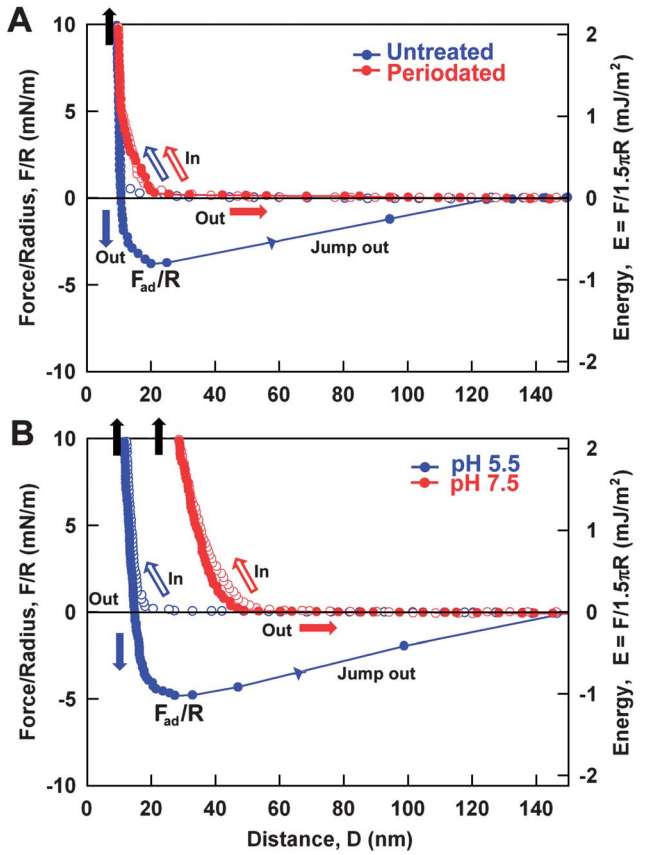

Fig. 2 Adhesion (F/R) and adhesion energy (E) changes between mcfp-1 films and TiO_2 surfaces (A) before and after periodate treatment ($NaIO_4$) at pH 5.5 (B) upon raising the pH from 5.5 to 7.5.

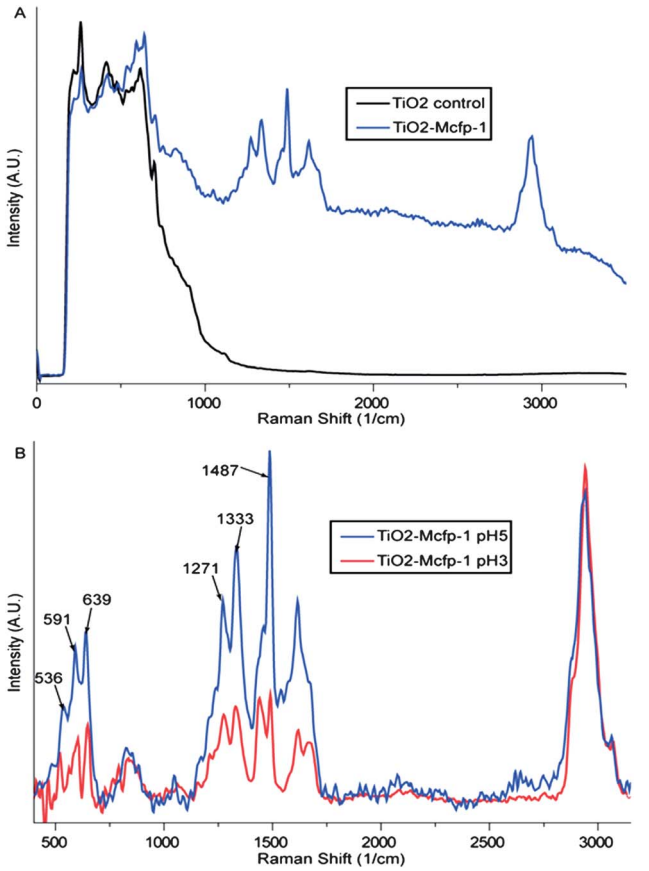

Fig. 3 Resonance Raman spectra of DOPA–TiO_2 interactions. (A) Raman spectra of mica coated with amorphous TiO_2 before (black line) and after (blue line) incubation with mcfp-1. (B) Background-subtracted spectra of DOPA–TiO_2 resonance for samples incubated at pH 5.0 (blue line) and pH 3.0 (red line). Resonance is reduced at lower pH relative to the non-resonant CH vibrational peak (2800–3100 cm^{-1}), but peaks signifying bidentate chelation are still apparent.

when mcfp-1 is incubated on the TiO_2 surface prior to measurement, several bands indicative of DOPA–metal coordination appear superimposed on the amorphous TiO_2 signal (Fig. 3A, blue line). Mcfp-1 incubated on untreated mica as a control shows no sign of the resonance peaks specific for catecholate–metal coordination (only fluorescence was observed; data not shown), strongly suggesting that the observed resonance bands acquired from the surface originate from the interaction of DOPA and TiO_2.

If the TiO_2/mica spectrum is subtracted (Fig. 3B), the positions of the background-corrected resonance peaks are consistent with many of the peaks arising from catechol–anatase adsorption,[23] as well as those originating from the complexation of mcfp-1 and Fe^{3+} (Table S1†).[10,11,24] The resonance peaks in the higher energy region of the spectra (1200–1500 cm^{-1}) were previously assigned to catechol ring vibrations, whereas the lower energy peaks (500–700 cm^{-1}) were assigned to vibrations of the oxygen–metal chelation bonds (Table S1†). In Raman studies of catechol adsorbed on anatase, the low energy peaks are obscured by the strong signal originating from the anatase lattice vibrations; however, such peaks are observed in solutions of tris-catecholato–Ti(IV)[23] and are consistent with analogous peaks seen in Raman spectra of mcfp-1–Fe^{3+} (Table S1†).[4,5,22] More specifically, the peaks at 591 cm^{-1} and 639 cm^{-1} indicate coordination by the oxygens on C_3 and C_4 of the catechol ring, respectively.[26] The third peak at 536 cm^{-1} represents a charge transfer (CT) band that is only present when both oxygen atoms participate in coordination, indicating that chelation between DOPA and the TiO_2 surface is primarily bidentate.[23,25,26] Recent Raman studies on polymer hydrogels stabilized with DOPA–Fe^{3+} cross-links demonstrated that the CT band decreases in intensity as pH is lowered, such that it contributes very little to the resonance spectrum at pH < 6, suggesting monodentate chelation.[27] It is, therefore, curious that all three peaks are observed in the mcfp-1–TiO_2 spectra incubated at pH values as low as 3 (Fig. 3B, red trace). However, this is consistent with other studies, which showed that bidentate adsorption of catechol to surfaces *via* chelation is favored in acidic solutions, whereas dissolved catechol species were found to contribute little to resonance Raman spectra in this pH range.[23,27,28]

Based on these factors, we feel confident that the observed resonance peaks arise from DOPA side chains in mcfp-1 adsorbed onto the surface *via* bidentate chelation with TiO_2 molecules. Previous computational modeling of the catechol–anatase interaction indicates that bidentate mononuclear chelation is energetically preferred over the binuclear "bridging" variant, particularly at defect sites in the lattice.[29] Consequently, Lana-Villarreal *et al.*[23] proposed an octahedral coordination geometry in which the oxygen molecules of each catechol fill two positions of the complex, while the remaining four positions are occupied by oxygens within the TiO_2 anatase lattice. Although we do not use anatase surfaces for our studies, we suggest a

similar structure for the interaction between DOPA side chains of mcfp-1 and the amorphous TiO_2 surface. However, this requires that unsaturated Ti surface sites with a pair of "dangling" bonds are available to the catechol side group.[23] Considering that our surface consists of amorphous TiO_2 with a more randomly arranged lattice structure, it seems likely that such unsaturated surface sites are available, even if this availability is patchy. The presence of a DOPA–TiO_2 coordination resonance Raman signal at the surface does not rule out the additional presence of DOPA side chains molecularly adsorbed *via* hydrogen bonding and van der Waals interactions. Lana-Villarreal *et al.*[23] concluded, based on their studies, that chelation was the dominant interaction between catechol and anatase at low pH; however, hydrogen bonding adsorption interactions between catechol and rutile TiO_2 (110) surfaces were recently visualized using scanning tunneling microscopy.[30] It is conceivable that this difference may arise from the difference in availability for suitable chelation sites in the rutile form *vs.* the anatase form of TiO_2; however, this is beyond the scope of this study. It remains to be determined to what degree each mode of adsorption (chelation *vs.* molecular adsorption) exists in our system; however, bidentate metal coordination between DOPA side chains and TiO_2 clearly provides a major contribution to the adhesion forces measured in our SFA studies.

Conclusions

The protective cuticle of the mussel byssus can potentially provide bio-inspiration for the design of hard and flexible coatings for various technical and biomedical applications. One of the secrets of this unusual biological material is the use of DOPA to form strong, yet reversible cross-links with metal ions such as Fe^{3+}. Here, we demonstrated using SFA and resonance Raman spectroscopy that the cuticle protein, mcfp-1, also adheres robustly, yet reversibly, to amorphous TiO_2 surfaces in hydrated environments *via* bidentate coordination complexes with the DOPA side groups. The use of TiO_2 in various biomedical applications is potentially complicated by biocompatibility issues, which might be solved using appropriate coating technologies. In light of our results, catechol-based coating strategies should be further pursued.

Acknowledgements

D.S.H. acknowledges the Marine Biomaterials Research Center grant from the Marine Biotechnology Program funded by the Ministry of Land, Transport and Maritime Affairs, Korea and the National Research Foundation of Korea Grant funded by the Korean Government (MEST) (NRF-C1ABA001-2011-0029960). M.J.H. and A.M. acknowledge support by the Alexander von Humboldt Foundation and the Max Planck Society. H. Z. and Q. L. acknowledge the support of a Discovery Grant Award from the Natural Sciences and Engineering Research Council of Canada (NSERC) and an NSERC RTI Grant Award (for a surface forces apparatus, SFA). J.H.W. acknowledges funding from the Human Frontier of Science.

Notes and references

1 M. Long and H. J. Rack, *Biomaterials*, 1998, **19**, 1621–1639.
2 E. M. Hetrick and M. H. Schoenfisch, *Chem. Soc. Rev.*, 2006, **35**, 780–789.
3 P. H. Chua, K. G. Neoh, E. T. Kang and W. Wang, *Biomaterials*, 2008, **29**, 1412–1421.
4 N. Holten-Andersen, G. E. Fantner, S. Hohlbauch, J. H. Waite and F. W. Zok, *Nat. Mater.*, 2007, **6**, 669–672.
5 N. Holten-Andersen, H. Zhao and J. H. Waite, *Biochemistry*, 2009, **48**, 2752–2759.
6 C. V. Benedict and J. H. Waite, *J. Morphol.*, 1986, **189**, 171–181.
7 K. E. Anderson and J. H. Waite, *J. Exp. Biol.*, 2000, **203**, 3065–3076.
8 S. W. Taylor, G. W. Luther and J. H. Waite, *Inorg. Chem.*, 1994, **33**, 5819–5824.
9 M. J. Sever, J. T. Weisser, J. Monahan, S. Srinivasan and J. J. Wilker, *Angew. Chem., Int. Ed.*, 2004, **43**, 448–450.
10 M. J. Harrington, A. Masic, N. Holten-Andersen, J. H. Waite and P. Fratzl, *Science*, 2010, **328**, 216–220.
11 H. Zeng, D. S. Hwang, J. N. Israelachvili and J. H. Waite, *Proc. Natl. Acad. Sci. U. S. A.*, 2010, **107**, 12850–12853.
12 S. T. Martin, J. M. Kesselman, D. S. Park, N. S. Lewis and M. R. Hoffmann, *Environ. Sci. Technol.*, 1996, **30**, 2535–2542.
13 J. L. Dalsin, L. Lin, S. Tosatti, J. Voros, M. Textor and P. B. Messersmith, *Langmuir*, 2005, **21**, 640–646.
14 H. Lee, N. F. Scherer and P. B. Messersmith, *Proc. Natl. Acad. Sci. U. S. A.*, 2006, **103**, 12999–13003.
15 J. J. Wang, M. N. Tahir, M. Kappl, W. Tremel, N. Metz, M. Barz, P. Theato and H. J. Butt, *Adv. Mater.*, 2008, **20**, 3872.
16 Q. Lin, D. Gourdon, C. Sun, N. Holten-Andersen, T. H. Anderson, J. H. Waite and J. N. Israelachvili, *Proc. Natl. Acad. Sci. U. S. A.*, 2007, **104**, 3782–3786.
17 T. H. Anderson, J. Yu, A. Estrada, M. U. Hammer, J. H. Waite and J. N. Israelachvili, *Adv. Funct. Mater.*, 2010, **20**, 4196–4205.
18 M. Benz, K. J. Rosenberg, E. J. Kramer and J. N. Israelachvili, *J. Phys. Chem. B*, 2006, **110**, 11884–11893.
19 B. Zappone, K. J. Rosenberg and J. Israelachvili, *Tribol. Lett.*, 2007, **26**, 191–201.
20 F. C. Teng, H. B. Zeng and Q. X. Liu, *J. Phys. Chem. C*, 2011, **115**, 17485–17494.
21 J. Yu, W. Wei, E. Danner, J. N. Israelachvili and J. H. Waite, *Adv. Mater.*, 2011, **23**, 2362–2366.
22 J. Yu, W. Wei, E. Danner, R. K. Ashley, J. N. Israelachvili and J. H. Waite, *Nat. Chem. Biol.*, 2011, **7**, 588–590.
23 T. Lana-Villarreal, A. Rodes, J. M. Perez and R. Gomez, *J. Am. Chem. Soc.*, 2005, **127**, 12601–12611.
24 S. W. Taylor, D. B. Chase, M. H. Emptage, M. J. Nelson and J. H. Waite, *Inorg. Chem.*, 1996, **35**, 7572–7577.
25 H. B. Yin, Y. Wada, T. Kitamura, S. Kambe, S. Murasawa, H. Mori, T. Sakata and S. Yanagida, *J. Mater. Chem.*, 2001, **11**, 1694–1703.
26 I. Michaud-Soret, K. K. Andersson, L. Que, Jr. and J. Haavik, *Biochemistry*, 1995, **34**, 5504–5510.
27 N. Holten-Andersen, M. J. Harrington, H. Birkedal, B. P. Lee, P. B. Messersmith, K. Y. C. Lee and J. H. Waite, *Proc. Natl. Acad. Sci. U. S. A.*, 2011, **108**, 2651–2655.
28 R. Rodriguez, M. A. Blesa and A. E. Regazzoni, *J. Colloid Interface Sci.*, 1996, **177**, 122–131.
29 P. C. Redfern, P. Zapol, L. A. Curtiss, T. Rajh and M. C. Thurnauer, *J. Phys. Chem. B*, 2003, **107**, 11419–11427.
30 S. C. Li, L. N. Chu, X. Q. Gong and U. Diebold, *Science*, 2010, **328**, 882–884.